British Journal of Pharmacology (2008) 153, 657–668

0007–1188/08 $30.00
www.brjpharmacol.org

RESEARCH PAPER

Inhibitors of histone deacetylase (HDAC) restore the p53 pathway in neuroblastoma cells

F Condorelli, I Gnemmi, A Vallario, AA Genazzani and PL Canonico

DiSCAFF&DFB Center, Università del Piemonte Orientale, Novara, Italy

Background and purpose: Inhibitors of histone deacetylase (HDAC) are emerging as a promising class of anti-cancer drugs, but a generic deregulation of transcription in neoplastic cells cannot fully explain their therapeutic effects. In this study we evaluated alternative molecular mechanisms by which HDAC inhibitors could affect neuroblastoma viability.
Experimental approach: Effects of HDAC inhibitors on survival of the I-type SK-N-BE and the N-type NB SH-SY5Y neuroblastoma cell lines were assessed by the MTT assay. Molecular pathways leading to this were examined by western blot, confocal microscopy and cytofluorometry. The mRNA levels of apoptotic mediators were assessed semi-quantitatively by RT-PCR. Tumour-suppressor p53 *trans* activity was assessed in EMSA experiments. HDAC inhibitors were also studied in cells subjected to plasmid-based p53 interference (p53i).
Key results: HDAC inhibitors induced cell death via the mitochondrial pathway of apoptosis with recruitment of Bcl-2 family members. Bcl-2 overexpression rendered neuroblastoma cells resistant to HDAC inhibitor treatment. Low concentrations of HDAC inhibitors (0.9 mM) caused a G_2 cell-cycle arrest and a marked upregulation of the p21/Waf1/Cip1 protein. HDAC inhibitors also activate the p53 protein via hyper-acetylation and nuclear re-localization, without affecting its protein expression. Accordingly, HDAC inhibitor-induced cell-killing and p21/Waf1/Cip1 upregulation is impaired in p53i-cells.
Conclusions and implications: In neuroblastoma cells, HDAC inhibitors may overcome the resistance to classical chemotherapeutic drugs by restoring the p53 tumour-repressor function via its hyper-acetylation and nuclear migration, events usually impaired in such tumours. In neuroblastoma cells, HDAC inhibitors are not able to induce p21/Waf1/Cip1 in the absence of a functional p53.
British Journal of Pharmacology (2008) **153,** 657–668; doi:10.1038/sj.bjp.0707608; published online 3 December 2007

Keywords: valproic acid; butyric acid; HDAC inhibitors; Bcl-2 pathways: anti- and proapoptotic; acetyl-p53

Abbreviations: Bcl-2, B-cell CLL/lymphoma 2 protein; BAX, Bcl-2-X antagonist of cell death protein; Bcl-X_L, Bcl-2 X analogue; HDAC, histone deacetylase; NOXA, phorbol-12-myristate-13-acetate-induced protein 1; PUMA, p53-upregulated modulator of apoptosis

Introduction

It is well established that tumour cells may acquire resistance to chemotherapeutic drugs through a variety of mechanisms, most of them implying an altered apoptotic programme (Lowe *et al*., 1993). Induction of apoptosis is in fact one of the mechanisms by which many 'new generation' anticancer therapies achieve their therapeutic effects (Barry *et al*., 1990; Sen and D'Incalci, 1992).

The main cellular molecules involved in this mechanism include overexpression of anti-apoptotic proteins such as B-cell chronic lymphocytic leukemia (CLL)/lymphoma 2 protein (Bcl-2) (Reed *et al*., 1991), silencing of inducers of apoptosis apoptotic peptidase activating factor-1(APAF-1) (Soengas *et al*., 2001) and mutations of the p53 protein (Lowe *et al*., 1993).

Correspondence: Dr F Condorelli, DiSCAFF & DFB center, Università del Piemonte Orientale 'A Avogadro', Via Bovio 6, Novara 28100, Italy.
E-mail: condorelli@pharm.unipmn.it
Received 14 June 2007; revised 26 July 2007; accepted 10 October 2007; published online 3 December 2007

In this regard, human neuroblastoma, the second most common solid tumour of childhood, exhibits a clinically and biologically heterogeneous behaviour, in part attributed to differential regulation of apoptosis and p53 response (Nicholson, 2000). For example, highly malignant and invasive neuroblastoma cell lines (N-type) were found resistant to apoptosis mediated by ligands of the cell-death family (such as TRAIL) by downregulating the expression of the initiator caspase-8 via gene hypermethylation and/or allelic deletion (Hopkins-Donaldson *et al*., 2000). In the same cell model, the activities of caspases can be inhibited further by inhibitors of apoptosis proteins, such as the X-linked inhibitors of apoptosis proteins (Igney and Krammer, 2002) and survivin (Adida *et al*., 1998) that, once overexpressed, prevent cell death by interacting with the apoptosome or effector caspases (caspase-3/7).

On the other hand, also the 'intrinsic' pathway of apoptosis, which relies on the activation of Bcl-2 family members with pro- and antiapoptotic regulatory functions,

may be disrupted in neuroblastoma cells by means of Bcl-2 overexpression (Fulda and Debatin, 2003).

p53 activation is found altered in neuroblastoma yet, unlike other tumour types, nearly all human neuroblastomas carry the wild-type (wt) *p53* gene (Komuro *et al*., 1993; Vogan *et al*., 1993) and wt p53 protein is expressed in many of the cell lines derived from neuroblastomas (Davidoff *et al*., 1992). On the other hand, in neuroblastomas, p53 protein is found to be restricted primarily to the cytoplasmic compartment (Moll *et al*., 1995). This suggests that the p53-mediated response in neuroblastoma cells is impaired because of an unknown cytoplasmic sequestration mechanism that prevents its translocation into the nucleus (Moll *et al*., 1995).

As deregulation of the p53 pathway in cell lines and in patient samples following chemotherapy is quite common and may contribute to drug resistance (Tweddle *et al*., 2001), existing antitumour therapy needs to be reinforced by the use of compounds able to bypass such impairment. In light of this, pharmacological inhibitors of histone deacetylase (HDAC) represent a new class of drugs, which allow a different therapeutic approach to cancer. Indeed, the local remodelling of chromatin and dynamic changes in the nucleosomal packaging, via acetylation/de-acetylation of core histone protein, play pivotal role in the regulation of accessibility to chromosomal DNA, and therefore on transcription. Among the most important regulators of such phenomena are specific enzymes that regulate N-terminal acetylation of lysine residues on H3 and H4 histones (Legube and Trouche, 2003), the histone acetyltransferases (HATs) and HDACs. These enzymes can be recruited to modify specific genes in complexes by sequence-specific transcription factors.

Valproic acid (VPA), widely used for the treatment of epilepsy and mood disorders (Bowden, 2003), is a short-chain fatty acid capable of eliciting numerous cellular responses such as deregulation of transcription. Indeed, beyond its therapeutic effect in neurological disorders, VPA was known to induce birth defects, when administered during pregnancy, such as incomplete neural tube closure and other malformations. Notably, valpromide (VPM), a closely related analogue, did not share this effect, leading to the proposal that HDAC inhibition could have important clinical potential (Phiel *et al*., 2001; Bowden, 2003). The ability of VPA to inhibit HDACs directly has been confirmed, and this compound displays an IC_{50} in the high micromolar range, compatible with its therapeutic efficacy (Gottlicher *et al*., 2001; Phiel *et al*., 2001).

Accordingly, VPA and the chemically related butyrate, both short-chain fatty acids, are emerging as critical regulators of cell growth, differentiation and apoptotic programmes in light of their ability to modulate gene transcription via regulation of histone acetylation (Heerdt *et al*., 1994; Mariadason *et al*., 1997; Gurvich *et al*., 2004). Concurrent with this effect on DNA packaging, a second mechanism by which HDACs may regulate gene expression is by regulating the acetylation of transcription factors (including p53, E2F and Sp3) whose de-acetylation has been linked to reduced DNA binding or transcriptional activity (Gu and Roeder, 1997; Marzio *et al*., 2000; Ammanamanchi *et al*., 2003). Furthermore, protein acetylation is emerging as a post-transcriptional modification determining the regulation of several signal-transduction pathways (Glozak *et al*., 2005). As a proof of their more general activity, it has been shown that HDAC inhibitors may activate the 'intrinsic' apoptosis via hyper-acetylation of Ku70 cytosolic protein, thus disrupting its binding to the pro-apoptotic Bcl-2 analogue, Bcl-2-X antagonist of cell death protein (BAX), and enabling its relocation to the mitochondria (Subramanian *et al*., 2005).

In the present paper, we have assessed the effects of butyrate and VPA treatment on neuroblastoma HDACs, intending to link their biochemical function to the biological effects. We used SH-SY5Y and SK-N-BE human neuroblastoma cell lines, representative of neuronal (I)-, more aggressive and intermediate (N)-histotype, which differ in terms of morphology, lineage differentiation and biological behaviour. We now report that butyrate and VPA, but not VPM, inhibit HDACs in a dose-dependent manner and this inhibition occurs at concentrations compatible with their clinical use. Treatment of cells with therapeutic concentrations of butyrate and VPA (0.9 mM) induced an increase of functional p21/Waf1/Cip1 cyclin-dependent kinase inhibitors, whereas higher concentrations (3 mM) induced an activation of the mitochondrial pathway of apoptosis via BAX, NOXA (phorbol-12-myristate-13-acetate-induced protein 1) and αPUMA (alpha p53-upregulated modulator of apoptosis) recruitment and Bcl-2 downregulation. Interestingly, either 'low' (0.9 mM) or 'high' (3 mM) concentrations of HDAC inhibitor were able to induce activation of the p53 pathway that preceded all the described molecular and biological events. Although no sign of p53 upregulation was detected, both butyrate and VPA, even at 0.3 mM concentration, were able to preserve acetylation of p53 on lysine residues 373 and 382, which is thought to stabilize p53 in its active conformation.

Materials and methods

Cell lines

The N-type neuroblastoma cell line SK-N-BE and the I-type neuroblastoma cell line SH-SY5Y (Ciccarone *et al*., 1989) were obtained from American Type Culture Collection (LGC Promochem, Teddington, UK) and cultured in 50% Dulbecco's modified Eagle's medium (DMEM) and 50% F-12 supplemented with 10% fetal bovine serum, 2 mM L-glutamine, penicillin (100 μg ml^{-1}) and streptomycin (100 μg ml^{-1}). The 293-derived PHOENIX packaging cells (kind gift of GP Nolan, Stanford University) were maintained in DMEM supplemented with 10% heat-inactivated FBS and 2 mM L-glutamine.

Retroviral preparation and infection

To overexpress Bcl-2 in neuroblastoma cells, the retroviral vector pLXSN (carrying the neomycin-resistance cassette) containing its cDNA was used (Cirinna *et al*., 2000). pLXSN-hbcl-2 was transfected in PHOENIX packaging cells by the calcium phosphate technique (Mammalian Profection Kit; Promega, Milan, Italy). Immediately before transfection, cells were treated with 25 μM chloroquine to increase transfection efficiency. At 12 h post-transfection, DMEM

was replaced with new medium, and cells were grown for an additional 24 h. Supernatants were collected, filtered through 0.45-μm-pore-size filters and supplemented with 4 μg ml^{-1} of polybrene just before the spin-infection procedure. Briefly, neuroblastoma cell lines (2×10^5 cells ml^{-1}) were treated with the virus-containing medium, plated in six-well plates, and centrifuged for 45 min at 600 *g* in a 32 °C prewarmed centrifuge. Cells were then incubated for 4 h at 32 °C, followed by a second cycle of centrifugation and incubation with fresh virus-containing medium as described above. At the end of the second cycle, the infectious supernatant was replaced with 50% DMEM and 50% F-12 medium and cells were incubated overnight at 37 °C. The following day, after a third cycle of centrifugation and incubation with fresh infectious supernatant, cells were cultured in regular medium for 16 h and plated in the presence of neomycin for pLXSN-hbcl-2 (2 μg ml^{-1}); colonies were then expanded to generate cell clones stably expressing hbcl-2.

Western blotting

Whole-cell extracts were obtained in a 1% Triton X-100 lysis buffer (10 mM Tris (pH 7.5), 150 mM NaCl, 5 mM EDTA (pH 8.0), supplemented with 1 mM phenylmethylsulphonyl fluoride, 0.2 M sodium orthovanadate, 0.2 M sodium fluoride and 1 × protease inhibitor cocktail (Complete; Roche Applied Science, Indianapolis, IN, USA). Western blotting was performed using anti-BAD (sc-7869), BID (sc-6538), Bcl-2 (sc-492), Bcl-2 X analogue (Bcl-X_L) (sc-7195), BAX (sc-493), p21 (sc-397), p27 (sc-528), αPUMA (sc-19187) (Santa Cruz Biotechnology Inc., Santa Cruz, CA, USA); anti-cytochrome *c* (cat. no. 556433) and anti-caspase 3 (cat. no. 51-9000064) (BD Biosciences, Milan, Italy); anti-β actin (clone AC-74) (Sigma-Aldrich Inc., Milan, Italy); anti-NOXA (IMG-349) (Imgenex Corp., San Diego, CA, USA); anti-p53 (2524) (Cell Signaling Technology Inc., Danvers, MA, USA); acetyl-p53 Lys372–382 (06-758) (Upstate Biotechnology, Lake Placid, NY, USA); GAP-43 (clone 7B10) (Invitrogen, Milan, Italy); βTubIII (MMS-435P) (Covance Inc., UK), all in tris-buffered saline (TBS) containing 2–5% non-fat milk and 0.1% Tween-20 for 1–2 h at room temperature. Samples were loaded on a polyacrylamide-sodium dodecyl sulphate gel for electrophoresis. For experiments on histone acetylation, acid extraction of proteins was performed from VPA, VPM or butyrate-treated SH-SY5Y or SK-N-BE cells on 16% polyacrylamide-sodium dodecyl sulphate electrophoresis gel and blotted with an anti-acetyl-H3 (06-599) antibody (Upstate Biotechnology). After washing, blots were stained with appropriate horseradish peroxidase-conjugated secondary antibody (GE Healthcare Ltd., Little chalfont, UK) and bands were visualized using enhanced chemiluminescence of SuperSignal West Pico reagents (Pierce Biotech, Rockford, IL, USA). The western blots were captured with Fluor-S MultiImager and Quantity One Software (Bio-Rad Inc., Milan, Italy) was used to analyse all the blots.

Mitochondrial subcellular fractions

Subcellular fractionations were obtained by lysing cells in buffer A (20 mM HEPES pH 7.6, 10 mM KCl, 1.5 mM $MgCl_2$, 0.1 mM EGTA pH 8.0, 0.1 mM EDTA, 1 mM dithiothreitol (DTT) and 250 mM sucrose) supplemented with a cocktail of protease inhibitors (Complete; Roche Applied Science), 1 mM phenylmethylsulphonyl fluoride, phosphatase inhibitors (0.2 mM sodium orthovanadate, 1 mM sodium fluoride) and homogenized (20 strokes through a G25-gauge syringe). Samples were centrifuged twice (750 *g* for 5 min) to remove nuclei and unlysed cells, and centrifuged again (10 000 *g* for 10 min) to obtain the heavy membrane (HM) fraction (pellet). The supernatant was centrifuged at 150 000 *g* for 1.5 h to obtain the cytosolic fraction. The HM fractions were solubilized in a solution containing 1% Triton X-100, 10 mM Tris-HCl (pH 7.4), 150 mM NaCl, 5 mM EDTA, supplemented as previously described and incubated on ice for 30 min.

Nuclear subcellular fractions

Cells were grown in 90-mm dishes, cultured and treated as described. To prepare the nuclear extracts, the cells were washed with cold phosphate-buffered saline (PBS) twice, and detached from plates by adding 1 ml of detachment buffer (150 mM NaCl, 1 mM EDTA, pH 8.0, 40 mM Tris, pH 7.6) for 5 min at room temperature. The cells were then transferred to microcentrifuge tubes and centrifuged at 300 *g* for 4 min at 4 °C. The supernatant was discarded, and the pellet was resuspended in 400 μl of cold buffer A (10 mM HEPES, pH 7.9, 10 mM KCl, 0.1 mM EDTA, 1 mM DTT, 0.5 mM phenylmethylsulphonyl fluoride, supplemented with phosphatase and protease inhibitors) and incubated on ice for 15 min. Nuclei were pelleted by centrifuging at 2800 *g* for 4 min at 4 °C and then resuspended in 50 mM HEPES, pH 7.9, 0.4 M NaCl, 1 mM EDTA and 1 mM DTT, supplemented with phosphatase and protease inhibitors. The mixture was shaken vigorously for 15 min at 4 °C, centrifuged at 15 000 *g* for 5 min and the supernatant was collected. The protein concentration was determined by the Bradford assay.

Cytochrome c *and p53 immuno-localization*

Cells were grown on 18 mm coverslips (Fisher Scientific, Houston, TX, USA) and incubated at 37 °C, in the presence of specified VPA and butyrate concentrations. Cells were fixed in PBS containing 4% paraformaldehyde for 15 min at room temperature, washed with PBS and then permeabilized in PBS containing 0.2% Triton X-100 for 5 min. Cells were washed and then incubated with 1:500 dilution of anti-cytochrome *c* (cat. no. 556432, BD, Milano, Italy) or with 1:250 dilution of p53 (Cell Signalling Technology Inc.) antibody in PBS for 1 h at 37 °C. After washing, cells were stained with 1:250 dilution of AlexaFluor488-conjugated donkey anti-mouse-IgG (Molecular Probes, Eugene, OR, USA) in PBS for 1 h at 37 °C. Then the coverslips were inverted and adhered to the glass slides using a mounting solution (DakoCytomation, Carpinteria, CA, USA). Images from fluorescence patterns of the cells were obtained using a Leika TCS-SP2 microscope (Leika, Milano, Italy), and processed as one-color images with Adobe Photoshop software (Mountain View, CA, USA). Black and white conversion is displayed in figures.

Apoptotic nuclei staining

For confocal-microscopy analysis of DNA integrity, neuroblastoma cell lines were plated on 12-mm glass

coverslips and maintained for proper length of time with different butyrate and VPA concentrations. DRAQ5 (Biostatus Ltd., Leicestershire, UK) DNA dye was used for nuclear staining of living cells as apoptotic marker. Briefly, the dye was added to cultured cells at 10 μM for 5 min followed by fixation in a 3.7% PBS/paraformaldehyde for 10 min at room temperature. Cells were washed twice with PBS, and mounted onto coverslip to be visualized with a confocal microscopy (He–Ne laser UV 633 nm), described elsewhere.

Measurement of diploid DNA content by flow cytometry

Cells were collected by using trypsinization. Measurement of DNA content was conducted after synchronization of cells in G_0/G_1 phase in 0.5% fetal calf serum-containing media for 16 h. Following incubation of cells in labelling solution (50 μg ml^{-1} propidium iodide in PBS containing 0.2% Triton X-100 and 10 μg ml^{-1} RNAse A) for 30 min, data were collected and analysed by using a fluorescence-activated cell sorter Vantage DIVA cytometer equipped with CELLQUEST software (BD Biosciences).

Thiazolyl blue tetrazolium bromide assay

Experiments were performed in Locke solution (134 mM NaCl, 5 mM KCl, 4 mM $NaHCO_3$, 10 mM HEPES (pH 7.6), 2.3 mM $CaCl_2$, 1 mM $MgCl_2$, 5 mM sucrose) with a final thiazolyl blue tetrazolium bromide (MTT) concentration of 250 μg ml^{-1}. In brief, cells were washed twice in Locke solution and then grown for 1 h with MTT at 37 °C. Reactions were then stopped and the crystals were solubilized in isopropyl alcohol/HCl before being read at 570 nm in a spectrophotometer.

Electrophoretic mobility shift assay

For DNA-binding assays, 2 μg of nuclear protein extracts (described in 'Nuclear subcellular fraction' section) from control and treated cells were incubated with 5 ng of the p53 consensus binding oligonucleotide, 5-TACAGAACATGTC TAAGCATGCTG-3, which was labelled with [^{32}P]ATP (NEN Inc., Milan, Italy). The binding reaction was carried out in 20 μl of DNA-binding buffer (20 mM Tris (pH 7.5), 50 mM KCl, 5 mM $MgCl_2$, 1 mM DTT, 0.5 mM EDTA, 10% glycerol, 0.5 mg of bovine serum albumin and 100 ng of poly(dA) · poly(dT) as nonspecific competitor DNA). Where indicated, 100 ng (20-fold excess) of specific unlabelled oligonucleotide was included in the reaction as a control for specificity. Cold probe was added to the reactions 20 min before the [^{32}P]ATP-labelled probe. After incubation at room temperature for another 30 min, the reactions were resolved on a 6% native polyacrylamide gel in 0.5 × TBE buffer (44.5 mM Tris base, 44.5 mM boric acid and 1 mM EDTA, pH 8.3) and run at 4 °C for 2 h, followed by autoradiography.

RT-PCR analysis of mRNA levels of p21, p27 and Bcl-2 family members

For reverse transcriptase (RT-PCR) analysis, 1 mg of total RNA was used as template for first-strand cDNA synthesis. PCR conditions and primers were as follows. Bcl-2: 363-bp amplified product, 24 cycles, annealing temperature of 58 °C, 2.25 mM $MgCl_2$, forward: 5-acttcgccgagatgtccagc-3, reverse: 5-tgtggcccagataggcacc-3; BAX: 308-bp amplified product, 24 cycles, annealing temperature of 58 °C, 2.25 mM $MgCl_2$, forward: 5-accaagaagctgagcgagtg-3, reverse: 5-acaaagatggtcacggtctgc-3; NOXA: 240-bp amplified product, 30 cycles, annealing temperature of 54 °C, 2.25 mM $MgCl_2$, forward: 5-GCAAGAACGCTCAACCGA-3, reverse: 5-TCAGATTCAGAAGTTTCTGC-3; αPUMA: 135-bp amplified product, 24 cycles, annealing temperature of 54 °C, 2.25 mM $MgCl_2$, forward: 5-ATGGCGGACGACCTCAAC-3, reverse: 5-CCTAATTGGGCTCCATCTCG-3; p21/Waf1/Cip1: 140-bp amplified product, 22 cycles, annealing temperature of 55 °C, 2.25 mM $MgCl_2$, forward: 5-GGACCTGTCACTGTCTT GTA-3, reverse: 5-GGACCTGTCACTGTCTTGTA-3; p27/Kip1: 450-bp amplified product, 24 cycles, annealing temperature of 57 °C, 2.25 mM $MgCl_2$, forward: 5-TAACCCGGGACTTGG AGAAG-3, reverse: 5-GCTTCTTGGGCGTCTGCTC-3; β-actin: 262-bp amplified product, 18 cycles, annealing temperature of 58 °C, 2.25 mM $MgCl_2$, forward: 5-acatccgcaaagacctgtacg-3, reverse: 5-agcatttgcggtggacgatgg-3. PCR products were electrophoresed on 1.2–2% agarose gel.

RNA interference

Post-transcriptional gene silencing was achieved by transiently transfecting the host cells with the pKD-p53-v1 plasmid (Upstate Biotechnology) encoding a p53-specific short hairpin RNA designed to be cleaved into mature small interfering RNA. Liposome-based transfection was performed by using the Metafectene-PRO reagent (Biontex, Munich, Germany), in accord with the manufacturer's instructions. In brief, 80–90% confluent cells were transfected with 4 μg of DNA (mock or pKD-p53-v1) in six-well plates. After 48 h from transfection, cells were either lysed for western blot analysis of p53 levels or plated in 24-well plates, treated with HDAC inhibitor and MTT assayed for cell viability (as already described elsewhere).

Data analysis

All results were expressed as mean ± s.e. Statistical analysis was performed by ANOVA. A P-value of $\leqslant 0.05$ was considered to be statistically significant.

Drugs

VPA and VPM were kindly provided by Sigma-Tau (Pomezia, Italy). Butyrate was purchased from Sigma-Aldrich Inc.

Results

HDAC inhibitors and cell viability

To study the molecular mechanisms underlying the effects of HDAC inhibitors (namely butyrate and VPA) on neuroblastoma cells, cell viability was assessed via the MTT assay in two different human cell lines, SK-N-BE and SH-SY5Y, exposed to increasing concentrations of the compounds.

As shown in Figure 1a, in the cell lines tested both 3 mM butyrate and 3 mM VPA were able to induce a striking reduction in cell viability. In view of this, we evaluated H3 histone acetylation to create a circumstantial link between the cytotoxic nature of these drugs and their activity as HDAC inhibitors. By blotting nuclear protein extracts with an anti-acetyl-H3-specific antibody, we detected a relevant signal, as early as 4 h after treatment, at the lowest concentration tested (that is 0.1 mM butyrate or VPA), consistent with the concentrations found in literature (Figure 1b). As expected, further increases in the concentrations of either HDAC inhibitor greatly enhanced the levels of H3 acetylation (peaking at 3 mM either for butyrate or VPA; Figure 1b). To address the specificity of this effect, we treated neuroblastoma cells with VPM, a structural analogue of VPA that shares its neurological uses (Isoherranen *et al*., 2003) but lacks inhibition of HDAC (Phiel *et al*., 2001). In the two cell lines tested, VPM, up to 9 mM, was significantly less potent in reducing cell viability, and totally ineffective on H3 histone acetylation (Figure 1b).

HDAC inhibitors and differentiation of neuroblastoma cell lines

To characterize further the effects of HDAC inhibitors, we investigated the potential of these drugs to affect neuroblastoma cell morphology (neuron-like projections in phase contrast microscopy) or molecular responses (increased neuronal markers, that is GAP-43, βIII-tubulin by western blot), relative to the effects of all-trans retinoic acid (10 μM), a well-known inducer of differentiation. In our hands, the HDAC inhibitors were unable to trigger morphologic changes (data not shown) or signs of differentiation (Figure 1c) even at the highest concentration tested (3 mM; data not shown) or after chronic administration with a lower dose (0.3 mM for up to 14 days). Given that, we decided to investigate the molecular pathways leading to the cytotoxic effects of HDAC inhibitors at a concentration of 3 mM, which induced the greatest H3 acetylation and the widest cytotoxic difference between VPA and VPM. In all the experiments described below, SH-SY5Y and SK-N-BE cells behaved similarly and graphical representations and numerical figures will therefore refer to SH-SY5Y cells only, which were representative of both cell lines.

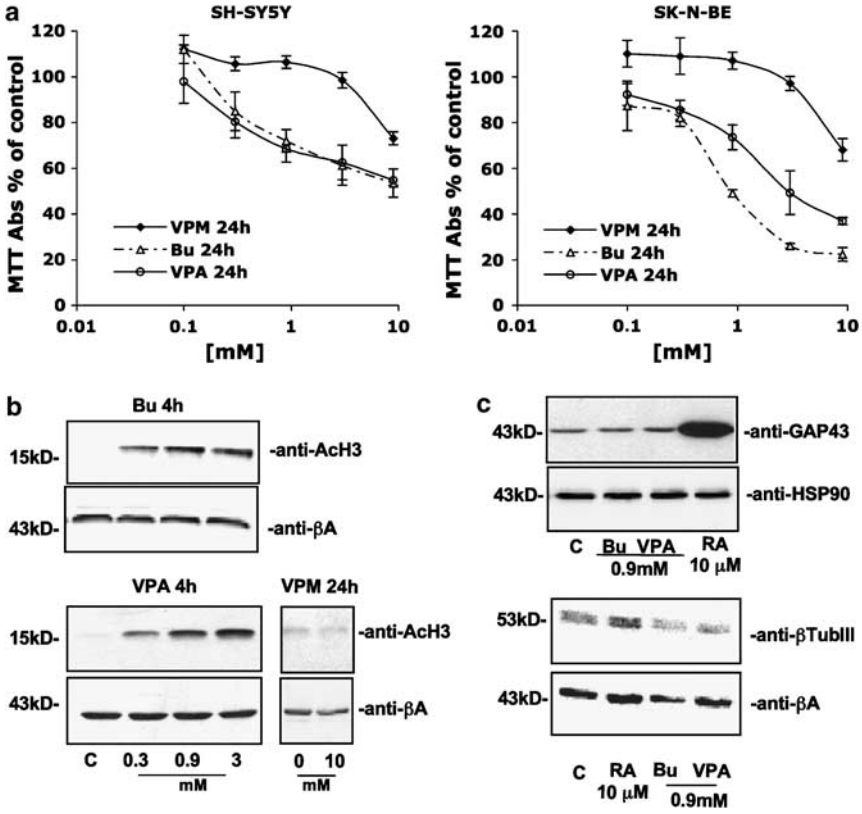

Figure 1 Characterization of the effects of HDAC inhibitors on human neuroblastoma cell lines. (**a**) Effect of 24 h treatment with VPM, butyrate (Bu) or VPA on SH-SY5Y and SK-N-BE neuroblastoma cell viability. Results (expressed as % surviving cells over respective control) represent the means ± s.e. of three different experiments performed in quadruplicate. (**b**) Butyrate and VPA, but not VPM, treatment enhanced the level of acetylated histone H3 protein in neuroblastoma cells. Cells were exposed for 4 h to HDAC inhibitors at final concentrations ranging between 0.3 and 3 mM. After treatment, proteins were extracted in acid conditions to improve nuclear fraction as described in Materials and methods, and 25 μg per lane was resolved on a polyacrylamide gel (15%). (**b**) VPM did not induce histone acetylation after 24 h exposure to the highest concentration tested (10 mM). (**c**) HDAC inhibitors did not affect neuroblastoma cell differentiation. GAP-43 or β-tubulin III (βTubIII) was chosen as molecular markers of differentiation. Retinoic acid (RA, 10 μM) treatment (48 h) was used as positive control of differentiation. (**b**, **c**) Western blot analysis of SH-SY5Y and SK-N-BE cells gave similar results.

Molecular characterization of cell death induced by HDAC inhibitors

To test whether apoptotic death was responsible for the effects measured in the MTT assay, cytosolic cytochrome *c* release and nuclear fragmentation, chosen as reliable markers of apoptosis, were assayed following butyrate or VPA treatment. As shown in Figure 2, HDAC inhibitors (3 mM) were able to induce nuclear fragmentation (fluorescence staining of DRAQ5-labelled cells after 24 h treatment; Figure 2A), which was chronologically preceded by cytochrome *c* release into the cytosol, as detected by both confocal microscopy (12 h; Figure 2B) and subcellular fractionation (12 h; Figure 2C).

Although Bcl-2 family members are the most relevant mediators of apoptosis in the mitochondrial compartment (Puthalakath and Strasser, 2002; Willis and Adams, 2005), we assumed they would have been modulated by HDAC inhibitors. We therefore monitored their protein expression after butyrate or VPA administration. Although no modulation of BAD, BID, BAX or BCL-X_L was observed (Figure 3a), a significant variation in Bcl-2, NOXA and αPUMA mRNA and protein levels was detected (Figures 3b and c). In detail, high concentrations of the HDAC inhibitors (3 mM), which elicited cell death (Figures 1a and 2a) and a sustained increase in histone acetylation (Figure 1b), significantly upregulated pro-apoptotic NOXA and αPUMA proteins,

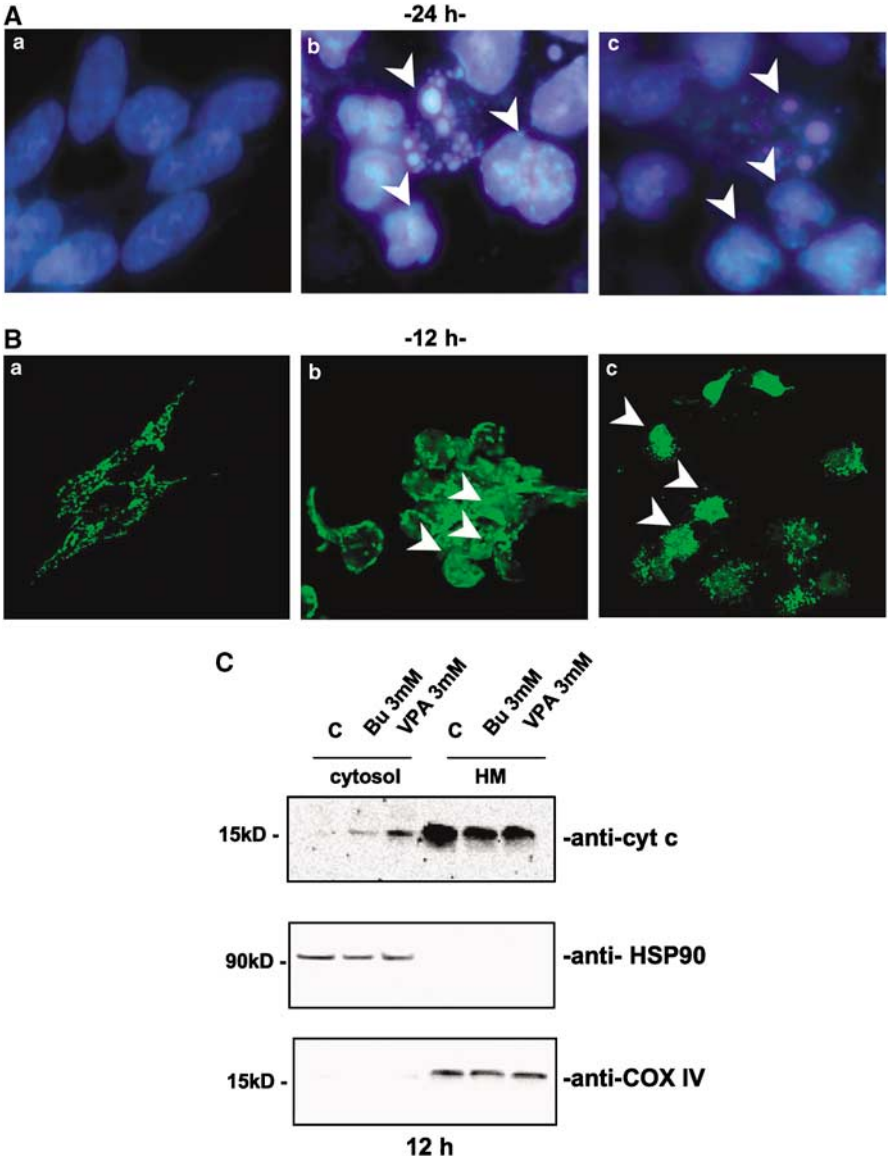

Figure 2 HDAC inhibitors induced a typical apoptotic death. (**A**) Nuclear fragmentation of neuroblastoma cells (SH-SY5Y) was assessed by fluorescent DNA staining. DRAQ5 nuclear dye showed the presence of fragmented, indented or condensed (arrows) nuclei only with the higher (**b**) butyrate or (**c**) VPA concentration (3 mM) used ((**a**) untreated control cells after 24 h in culture). (**B**) Confocal microscopy of cytochrome *c* (cyt *c*) mitochondrial de-localization (arrows) in SH-SY5Y following 12 h treatment with 3 mM (**b**) butyrate (Bu) or (**c**) VPA treatment and (**a**) control cells. (**C**) Western blot analysis of cytochrome *c* localization following subcellular fractionation (cytosol: soluble cytosolic fraction, 25 μg per lane; HM: heavy membrane fraction, 10 μg per lane) of SH-SY5Y neuroblastoma cells treated with Bu or VPA (12 h incubation). Heat-shock protein-90 (HSP-90) and cytochrome oxidase subunit IV (COX-IV) were evaluated as housekeeping proteins for cytosolic (HSP-90) or mitochondrial (COX-IV) fractions. Experiments on SK-N-BE cells gave similar results.

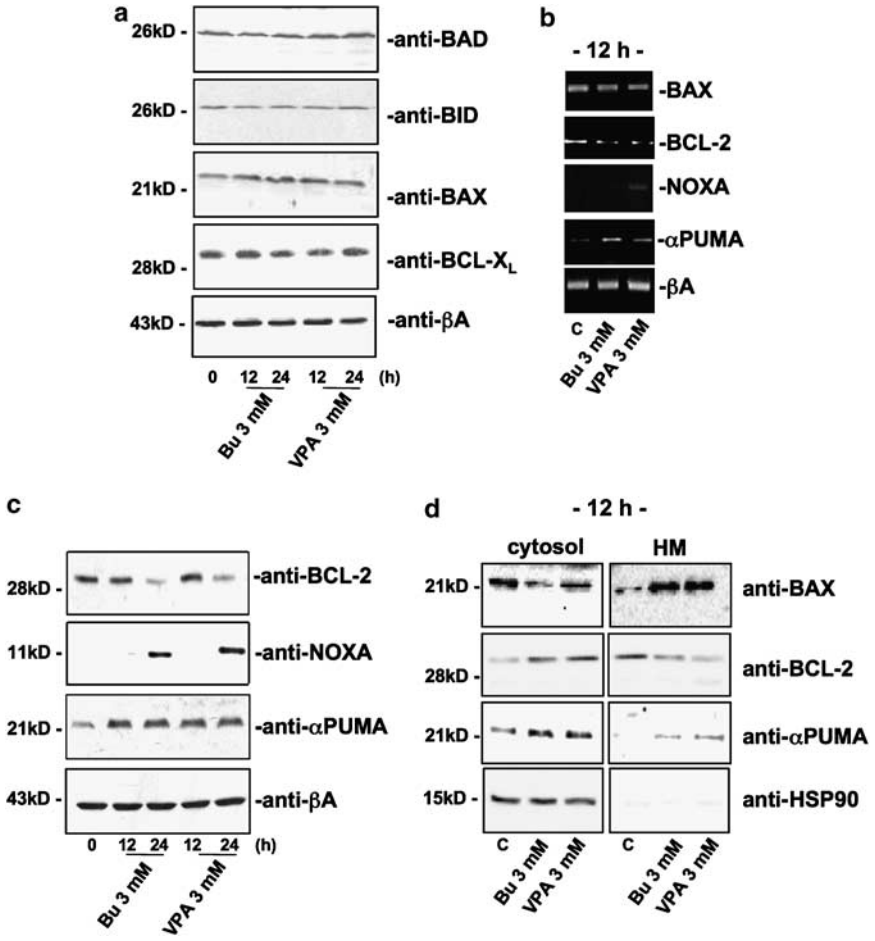

Figure 3 Expression of the Bcl-2 family proteins in SH-SY5Y neuroblastoma cells treated with butyrate (Bu) or VPA for 12 or 24 h. (**a**, **c**) Western blot analysis of whole extracts with the specified antibodies (25 μg per lane of proteins). β-Actin levels were assessed as a proof of equal loading for each panel (data not shown). (**b**) RT-PCR analysis of BAX, Bcl-2, NOXA and αPUMA mRNA levels after 12 h of butyrate or VPA treatment. β-Actin mRNA levels were evaluated to equalize the amount of cDNA amplified by PCR. Experiments on SK-N-BE cells gave similar results. (**d**) BAX, αPUMA and Bcl-2 subcellular localization after HDAC inhibitor treatment (cytosol: soluble cytosolic fraction, 25 μg per lane; HM: heavy membrane fraction, 10 μg per lane). Heat-shock protein-90 (HSP-90), which has an exclusive cytosolic localization, was assessed in the mitochondrial compartment (HM) as a control for good quality subcellular fractionation (data not shown).

while downregulating the anti-apoptotic Bcl-2 protein (Figure 3c). Interestingly, αPUMA levels were increased within the first 12 h after treatment, whereas NOXA and Bcl-2 modulation were delayed.

To evaluate whether or not the HDAC inhibitors may modulate the re-localization of Bcl-2 and its protein homologues, we blotted subcellular protein fractions (cytosol vs mitochondria) of treated or untreated cells with Bcl-2-, BAX-, NOXA- and αPUMA-specific antibodies. As shown in Figure 3d, butyrate and VPA (3 mM) were able to induce BAX and PUMA mitochondrial localization after 12 h while, simultaneously, lowering Bcl-2 in this compartment. Concomitantly, BID, BAD and BCL-X_L, which were not modulated in their expression, did not modify their subcellular localization following HDAC inhibitors administration.

In the same experimental conditions, Bcl-2, BAX, NOXA and αPUMA mRNAs were monitored, by the semiquantitative RT-PCR assay, in response to treatment with HDAC inhibitors. The profile of changes in mRNA levels matched that of changes in protein (western blots), although the mRNA changes took place at earlier times of exposure to HDAC inhibitors (Figure 3b). Particularly, Bcl-2 mRNA was significantly downregulated as early as 12 h after treatment with HDAC inhibitors (3 mM).

The role of Bcl-2 in the neuroblastoma cell response to HDACi treatments

The biological relevance of the downregulation of Bcl-2 induced by HDAC inhibitors (3 mM butyrate or VPA) was further investigated in Bcl-2 overexpressing cells. Figure 4 shows that Bcl-2 overexpressing cells displayed a marked reduction in sensitivity to HDACi-induced cytotoxicity in both SH-SY5Y and SK-N-BE cell lines. In these cells, HDAC inhibitors at 3 mM induced the same level of cell death as obtained with 10-fold lower concentrations in mock-transfected cells.

HDAC inhibitors and neuroblastoma cell-cycle distribution

To better characterize the effects of HDAC inhibitors on neuroblastoma cell cycling, we evaluated the DNA content

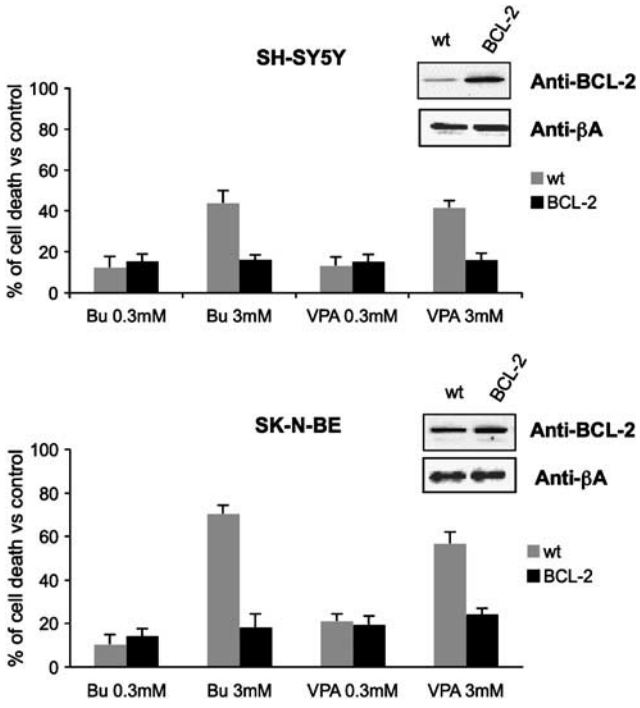

Figure 4 Viability of wild-type (wt) and overexpressing Bcl-2 (BCL-2) SH-SY5Y and SK-N-BE cells treated for 24 h with different butyrate (Bu) or VPA concentrations. Results (expressed as % cell death vs untreated controls) represented the means ± s.e. of three different experiments performed in quadruplicate.

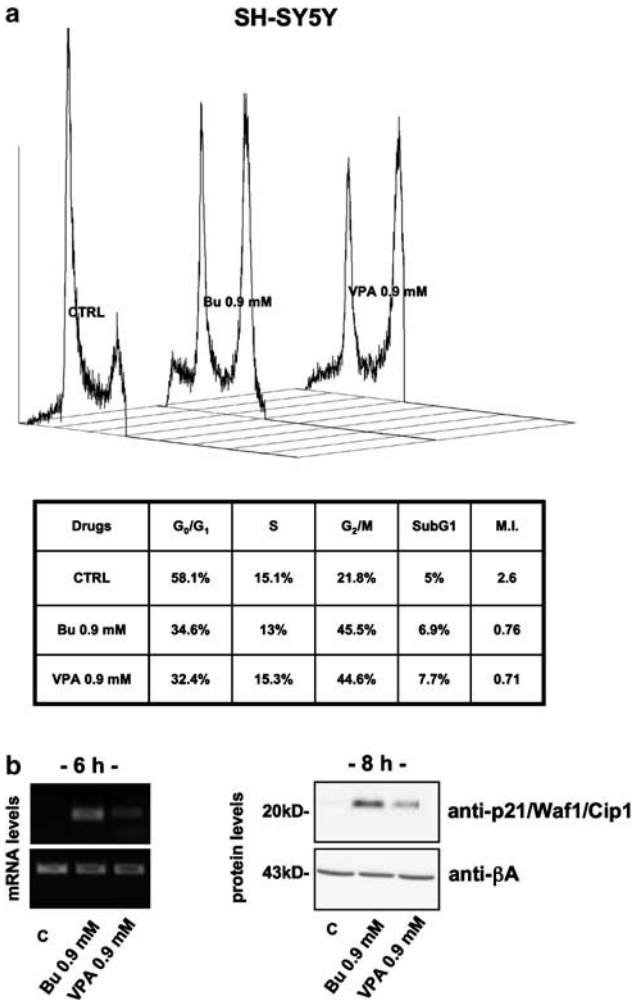

Drugs	G_0/G_1	S	G_2/M	SubG1	M.I.
CTRL	58.1%	15.1%	21.8%	5%	2.6
Bu 0.9 mM	34.6%	13%	45.5%	6.9%	0.76
VPA 0.9 mM	32.4%	15.3%	44.6%	7.7%	0.71

Figure 5 Cell-cycle distribution and expression of p21/Waf1/Cip1 in SH-SY5Y neuroblastoma cells treated with butyrate (Bu) or VPA. (**a**) Cell-cycle distribution of HDAC inhibitor-treated neuroblastoma cells. Cells were synchronized by serum deprivation for 16 h before butyrate or VPA treatment (16 h). Values represent percentages of phase-specific populations. MI is the product of G_1/G_2 ratio. (**b**) RT-PCR analysis of relative mRNA levels after 6 h treatment (left) and western blot analysis (right) of protein expression (30 μg per lane of proteins) after 8 h in the presence of butyrate or VPA (0.9 mM). β-Actin mRNA and protein levels were evaluated as a proof of equal loading. All the experiments on SK-N-BE cells gave similar results.

of butyrate- or VPA-treated cells after propidium iodide staining by cytofluorometry (Figure 5a). For these experiments, we decided to use HDAC inhibitors at 0.9 mM, a concentration that was able to consistently reduce cell viability (about 30% vs untreated controls, depending on the cell type). Higher concentrations (3 mM) were not considered because of their intrinsic cytotoxic effect, which may result in misinterpretation of cell-cycle data (cellular debris and hypoploid population discrimination).

Interestingly, both butyrate and VPA markedly affected cell-cycle distribution, causing a G_2 block with a clear reduction in the G_1-phase population. This redistribution along the different steps of cell cycle inverted the G_1/G_2 ratio (mitotic index) of SH-SY5Y cells from 2.6 in untreated cells to 0.76 (with butyrate 0.9 mM) and 0.71 (with VPA 0.9 mM) after 16 h HDACi administration. Results of the same order were obtained in SK-N-BE cells (data not shown).

Characterization of a functional p53 pathway in neuroblastoma cell lines

As the cell-cycle profiles of HDAC inhibitor-treated cells closely resembled those of cells poisoned with p53-targeting drugs (for example, doxorubicin, gemcitabine), we evaluated the protein levels of the well-known cyclin-dependent kinase inhibitor, p21/Waf1/Cip1, a downstream target for p53. As expected, butyrate and VPA were able to increase both mRNA and protein levels of p21, as measured by RT-PCR and western blot, already after 6 h (mRNA) or 8 h (protein) of treatment (Figure 5b). Accordingly, we looked for the activation of a typical p53 pathway. After treatment with 3 mM HDAC inhibitors, whole or nuclear protein extracts were collected to evaluate total levels of p53 and its subcellular distribution by western blot. As shown in Figure 6, HDAC inhibitors, even though ineffective on the total levels of p53 (Figure 6a), were able to induce its nuclear translocation as soon as 4 h (Figure 6b). Nuclear translocation was associated with an enhanced trans activity of p53 as demonstrated by electromobility shift assay experiments (Figure 6c) in which both butyrate and VPA caused p53 to specifically bind its consensus DNA. Moreover, the HDAC inhibitors were able to induce hyper-acetylation of p53. Indeed, by probing neuroblastoma cytosolic vs nuclear fractions with an anti-acetyl p53-specific antibody (lysine

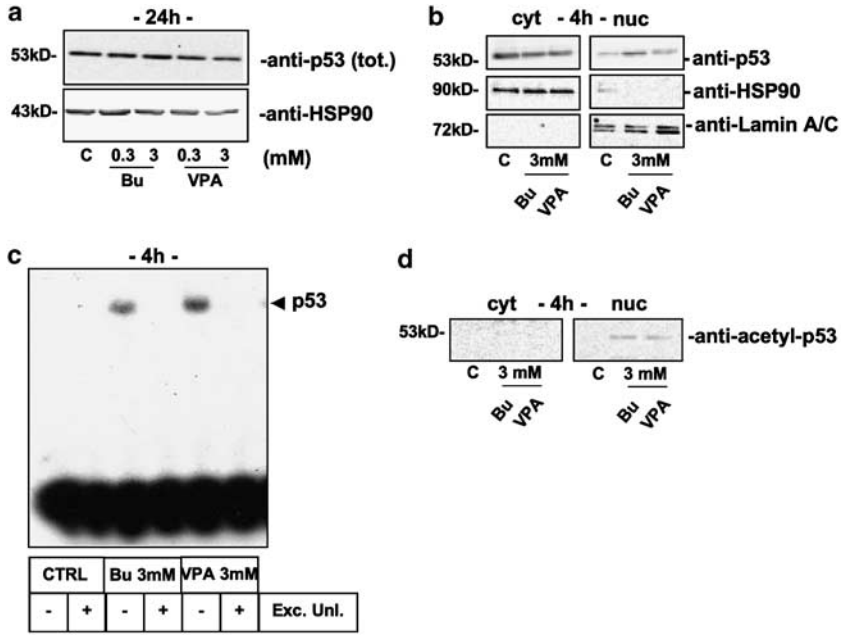

Figure 6 Activation of the p53 pathway in SH-SY5Y neuroblastoma cells treated with butyrate (Bu) or VPA. (**a**) Western blot analysis of p53 levels in whole extracts (40 μg per lane of proteins) after 24 h treatment in the presence of low (0.3 mM) or high (3 mM) concentrations of HDAC inhibitor. (**b**) Cytosolic (cyt, 40 μg per lane of proteins) vs nuclear (nuc, 7.5 μg per lane) distribution of p53 after 4 h treatment with 3 mM butyrate or VPA (upper panel). Heat shock protein-90 (HSP-90; middle panel) and Lamin A/C (lower panel) were evaluated as a proof of purity and equal loading for cytosolic (HSP-90) or nuclear (Lamin A/C) extracts. (**c**) Electromobility shift assay experiment with p53-specific probe after butyrate and VPA treatment using 2 μg of nuclear extracts. The specificity of p53 binding was assessed by performing the experiment in duplicate with the labelled probe alone or by adding 20-fold excess of unlabelled probe (Exc. Unl.). (**d**) Western blot analysis of p53 lysine (373 and 382) acetylation in cytosolic (cyt, 40 μg per lane of proteins) vs nuclear (nuc, 7.5 μg per lane) subcellular fractions. Total levels of p53 in the cytosolic and nuclear compartments are displayed in (**b**). Experiments on SK-N-BE cells gave similar results.

373 and 382), we detected a reactive band in cells treated with HDAC inhibitors, specifically in the nuclear compartment (Figure 6d).

p53 expression and neuroblastoma cells response to HDAC inhibitors

SH-SY5Y and SK-N-BE cell lines depleted the p53 protein (SH-p53 interference (p53i) and SK-p53i, respectively) by transient transfection of a plasmid encoding a p53-specific short hairpin RNA displayed an altered response to treatment with HDAC inhibitors. As shown in Figure 7a, this approach allowed us to obtain mixed populations of cells whose p53 content was decreased by approximately 60% (SY) and 40% (SK) compared with mock-transfected cells. In this condition, p53i cells proved to be more resistant to HDAC inhibitor-induced killing (MTT assay), especially at the 0.3 and 0.9 mM concentrations (Figure 7b). In the same cells, induction of p21/Waf1/Cip1 by HDAC inhibitors was also prevented (Figure 7c).

Discussion

It has been shown that HDAC inhibitors may be pro-differentiative (Hall *et al*., 2002) and/or pro-apoptotic (Kawagoe *et al*., 2002) depending on the cell type considered, suggesting that HDACs might represent a relevant target for cancer therapy (Marks *et al*., 2001). In partial agreement with this, human neuroblastoma cell lines, at least in our hands, were found responsive to HDAC inhibitor treatment as their viability was reduced in a dose- and time-dependent fashion. However, in contrast to previously reported data from other groups (Yuan *et al*., 2001; Hao *et al*., 2004; Laeng *et al*., 2004), no molecular (increased expression of βIII-tubulin or GAP-43) or morphological (axon-like sprouting) signs of differentiation were detected in all the culture conditions tested (HDAC inhibitors acutely or chronically administered).

The reduced viability in neuroblastoma cells was likely to depend on the induction of apoptotic death, as suggested by mitochondrial cytochrome *c* release and nuclear DNA fragmentation. These observations, therefore, suggest that HDAC inhibitor-induced apoptosis is likely to proceed via the mitochondrial pathway. At the same time, this does not exclude the release of other cell-death effectors, such as apoptosis-inducing factor (Susin *et al*., 1999) and endonuclease G (Widlak and Garrard, 2005), by mitochondria, as we observed for cytochrome *c* (Figures 2b and c).

It has been widely accepted that the mitochondrial activation is crucial in several models of apoptosis (Waterhouse *et al*., 2002). In these organelles, the balance between the actions of pro-death (BAX, BID, NOXA, αPUMA and BAD among others) or pro-life (mainly Bcl-2 and BCL-X_L) members of the Bcl-2 family determines whether or not pro-apoptotic mediators (such as cytochrome *c*) have to be released from the mitochondria (Puthalakath and Strasser, 2002; Willis and Adams, 2005). In our model, HDAC inhibitors were found to affect the expression and distribution of some of these Bcl-2

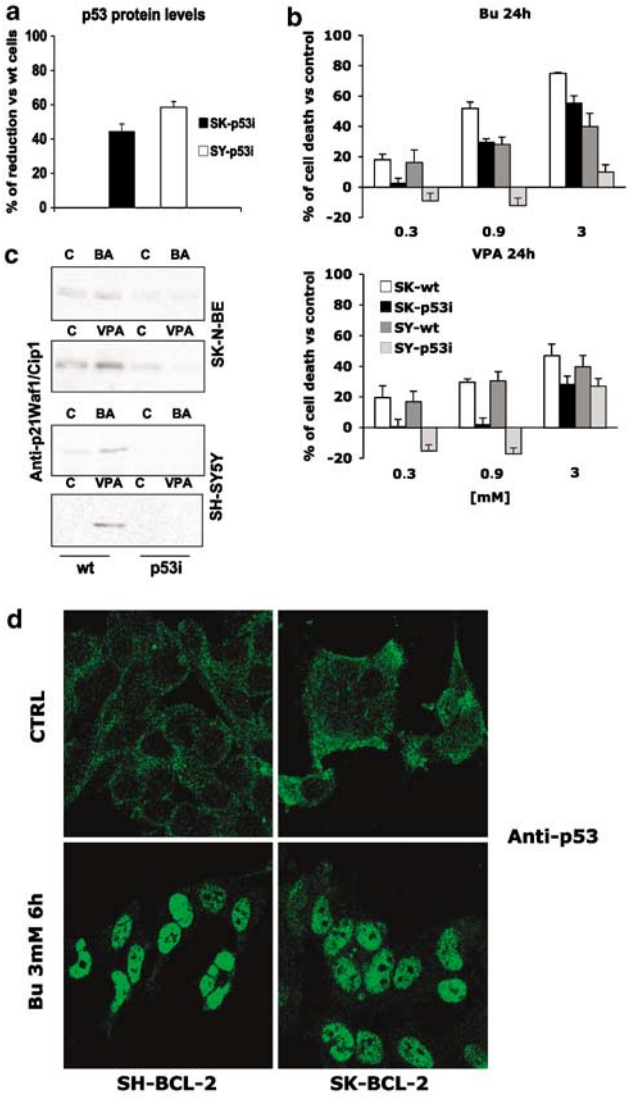

Figure 7 p53 dependence of HDAC inhibitor-induced effects. (**a**) Densitometric analysis of p53 interference (p53i) vs SH-SY5Y and SK-N-BE parental cell lines. Absorbance values of western blot p53-reactive bands from p53i cells were corrected for the β-actin values (internal standard) compared with the values obtained from parental cell lines and expressed as % of reduction. (**b**) Cell death of wild-type (wt) and p53i SH-SY5Y and SK-N-BE cells treated for 24 h with different butyrate or VPA concentrations. Results (expressed as % cell death vs untreated controls) represent the means ± s.e. of three different experiments performed in quadruplicate. (**c**) Western blot analysis of p21/Waf1/Cip1 expression in wt and p53i SH-SY5Y and SK-N-BE cells following HDAC inhibitor treatment (0.9 mM, 8 h). (**d**) Bcl-2 overexpression did not affect HDAC inhibitor-induced p53 nuclear translocation. Parental SH-SY5Y and SK-N-BE cell lines or their Bcl-2 overexpressing derivatives were treated with butyrate (0.9 mM) for 6 h and p53 subcellular localization was studied by confocal microscopy with an anti-p53-specific antibody. Similar results were obtained after VPA treatment (not shown).

homologues such as BAX, NOXA, αPUMA and Bcl-2 itself. Particularly, the increase in αPUMA levels (detectable after 12 h treatment) preceded the modification of NOXA and Bcl-2 proteins (16 h), an observation apparently in contrast to the timing of cytochrome *c* release (already significant after 12 h). In our opinion, this discrepancy in the schedule of the molecular events that lead to the apoptotic death may suggest that, while αPUMA takes part in the induction of this process, the modulation of NOXA and Bcl-2 expression serves as an amplifier to the cytotoxic effects of HDAC inhibitors.

In the same experimental settings, VPM failed to modulate Bcl-2 family members at all concentrations tested, thereby reinforcing the hypothesis that these effects are a consequence of the inhibition of deacetylase enzymes. It is also important to mention that similar results, in terms of timing of modulation, were obtained in SK-N-BE cells, thus suggesting a more general, not cell-line specific, mechanism of action for HDAC inhibitors.

Also, the subcellular localization of Bcl-2 and its parental proteins in response to HDAC inhibitors was in agreement with the hypothesis of a mitochondrial-dependent apoptotic death. Indeed, both butyrate and VPA (3 mM) caused mitochondrial localization of BAX and PUMA, simultaneously lowering Bcl-2 in the same compartment. These data seem to link the re-localization of pro-apoptotic Bcl-2 members tightly to cytochrome *c* release based on the lag-time required for both events to occur (within 12 h after treatment). The weak mitochondrial localization of the anti-apoptotic Bcl-2 in butyrate- and VPA (3 mM)-treated cells, in fact, represents a condition in which Bcl-2 would not be able to counteract the rise in BAX and NOXA, thus reinforcing the stimulus for cytochrome *c* release. Moreover, these experiments suggest that BAX, although not upregulated at the transcriptional level, might be activated in HDAC inhibitor-induced apoptosis. This hypothesis is supported by other groups who have linked the mitochondrial translocation of BAX to the hyper-acetylation of Ku70, which normally retains BAX in the cytosol (Subramanian *et al*., 2005).

It is also important to notice that Bcl-2 mRNA was significantly downregulated already after 12 h treatment with HDAC inhibitors (3 mM) and this, considering its long half-life (Schiavone *et al*., 2000), suggests that HDAC inhibitors may induce a 'factor' responsible for Bcl-2 down-regulation. The relevance of Bcl-2 in the response of neuroblastoma to HDAC inhibitors was further demonstrated in cell lines overexpressing this protein.

In parallel, at a concentration (0.9 mM) lower than those required for cell death to occur (3 mM), the HDAC inhibitors were able to cause G_2 block of the cell cycle and induction of the p21 protein a target for p53. The concurrent upregulation of p21/Waf1/Cip1, NOXA and αPUMA, three genes normally trans-activated by the tumour-suppressor gene p53 (Waga *et al*., 1994; Culmsee and Mattson, 2005), led us to demonstrate that the HDAC inhibitors are able to activate the p53-pathway in neuroblastoma cell lines. Notably, such activation was not due to an increase in p53 protein levels but to its hyper-acetylation, which is thought to stabilize its nuclear active form (Legube *et al*., 2004). This latter finding supports the observation of Zhao *et al*. (2006) that HDAC inhibitor-triggered activation of p53 pathways is a consequence of p53 hyper-acetylation instead of an induction of protein levels, and are particularly relevant considering that neuroblastomas are usually characterized by the presence of a sequestered cytoplasmic form of p53 (inactive), which may account for their chemoresistance (Moll *et al*., 1995).

The centrality of p53 in the effects of HDAC inhibitors was strengthened by the experiments with SK and SY cells in which p53 levels were reduced via RNA interference. Under these experimental conditions, SY cells became more resistant to HDAC inhibitors, a finding compatible with the greater effect of p53 knockout in SY than in SK cells.

The demonstration of p53 activation by HDAC inhibitors is also of importance in another respect. There are several reports in the literature linking the rise in p21/Waf1/Cip1 levels to a histone-directed effect of HDAC inhibitors (Gottlicher *et al*., 2001) but, in contrast to these reports, our results definitely associated the activation of the cyclin-dependent kinase inhibitor with the presence of a functional p53 protein. Such findings were also supported by the observations made in the GIMEN human neuroblastoma cell line, which express very low levels of p53, comparable to those in p53i SK and SY cells. The GIMEN cells were totally resistant to treatment with HDAC inhibitors, at concentrations up to 3 mM (data not presented).

In conclusion, in two neuroblastoma cell lines, HDAC inhibitors were able to induce apoptotic cell death involving the mitochondrial pathway. The apoptotic programme is likely to rely on BAX, NOXA and αPUMA activation, and Bcl-2 downregulation. Moreover, Bcl-2 was reduced, thus implying activation of a pathway controlling its degradation. Interestingly, the involvement of the mitochondrial pathway, which is downstream of the activation of the p53 tumour-suppressor gene, relies on its hyper-acetylation. Indeed, cells overexpressing Bcl-2 were more resistant to HDAC inhibitor treatment, without affecting p53 nuclear localization (Figure 7d). Thus, HDAC inhibitors may not only affect HDAC but may also be more promiscuous inhibitors of deacetylase enzymes modulating the acetylation status of other proteins such as p53. This alternative mechanism for HDAC inhibitors seems to be common to those neuroblastoma cell line expressing a functional p53 (SK-N-BE and SH-SY5Y), and clearly relies on its expression (no effect in the p53-depleted GIMEN cell line). We did not test whether an HDAC inhibitor-induced, p53-dependent pathway is present in other cancer cell lines nor in normal neuroblasts, but there is growing evidence that this might be a more generalized event (Savickiene *et al*., 2006; Zhao *et al*., 2006). More relevantly, the HDAC inhibitor-induced upregulation of p21/Waf1/Cip1 has to be linked to their ability to activate a canonical p53 pathway.

To our knowledge, this is the first demonstration of an HDAC inhibitor-dependent activation of the p53 pathway in neuroblastoma cells known for an abnormal p53 function that is responsible for their resistance to chemotherapy. As a consequence of this ability to restore p53 function, we consider HDAC inhibitors to be a promising class of drugs for the treatment of chemoresistant neuroblastoma tumours.

Acknowledgements

This study was supported in part by a grant from Sigma-Tau, Pomezia, Italy and from University grants (PRIN 2004) to PLC and FC.

Conflict of interest

FC and PLC have received unrestricted grants from Sigma-Tau, Pomezia, Italy.

References

Adida C, Berrebi D, Peuchmaur M, Reyes-Mugica M, Altieri DC (1998). Anti-apoptosis gene, survivin, and prognosis of neuroblastoma. *Lancet* **351**: 882–883.

Ammanamanchi S, Freeman JW, Brattain MG (2003). Acetylated sp3 is a transcriptional activator. *J Biol Chem* **278**: 35775–35780.

Barry MA, Behnke CA, Eastman A (1990). Activation of programmed cell death (apoptosis) by cisplatin, other anticancer drugs, toxins and hyperthermia. *Biochem Pharmacol* **40**: 2353–2362.

Bowden CL (2003). Valproate. *Bipolar Disord* **5**: 189–202.

Ciccarone V, Spengler BA, Meyers MB, Biedler JL, Ross RA (1989). Phenotypic diversification in human neuroblastoma cells: expression of distinct neural crest lineages. *Cancer Res* **49**: 219–225.

Cirinna M, Trotta R, Salomoni P, Kossev P, Wasik M, Perrotti D *et al.* (2000). Bcl-2 expression restores the leukemogenic potential of a BCR/ABL mutant defective in transformation. *Blood* **96**: 3915–3921.

Culmsee C, Mattson MP (2005). p53 in neuronal apoptosis. *Biochem Biophys Res Commun* **331**: 761–777.

Davidoff AM, Pence JC, Shorter NA, Iglehart JD, Marks JR (1992). Expression of p53 in human neuroblastoma- and neuroepithelioma-derived cell lines. *Oncogene* **7**: 127–133.

Fulda S, Debatin KM (2003). Apoptosis pathways in neuroblastoma therapy. *Cancer Lett* **197**: 131–135.

Glozak MA, Sengupta N, Zhang X, Seto E (2005). Acetylation and deacetylation of non-histone proteins. *Gene* **363**: 15–23.

Gottlicher M, Minucci S, Zhu P, Kramer OH, Schimpf A, Giavara S *et al.* (2001). Valproic acid defines a novel class of HDAC inhibitors inducing differentiation of transformed cells. *EMBO J* **20**: 6969–6978.

Gu W, Roeder RG (1997). Activation of p53 sequence-specific DNA binding by acetylation of the p53 C-terminal domain. *Cell* **90**: 595–606.

Gurvich N, Tsygankova OM, Meinkoth JL, Klein PS (2004). Histone deacetylase is a target of valproic acid-mediated cellular differentiation. *Cancer Res* **64**: 1079–1086.

Hall AC, Brennan A, Goold RG, Cleverley K, Lucas FR, Gordon-Weeks PR *et al.* (2002). Valproate regulates GSK-3-mediated axonal remodeling and synapsin I clustering in developing neurons. *Mol Cell Neurosci* **20**: 257–270.

Hao Y, Creson T, Zhang L, Li P, Du F, Yuan P *et al.* (2004). Mood stabilizer valproate promotes ERK pathway-dependent cortical neuronal growth and neurogenesis. *J Neurosci* **24**: 6590–6599.

Heerdt BG, Houston MA, Augenlicht LH (1994). Potentiation by specific short-chain fatty acids of differentiation and apoptosis in human colonic carcinoma cell lines. *Cancer Res* **54**: 3288–3293.

Hopkins-Donaldson S, Bodmer JL, Bourloud KB, Brognara CB, Tschopp J, Gross N (2000). Loss of caspase-8 expression in neuroblastoma is related to malignancy and resistance to TRAIL-induced apoptosis. *Med Pediatr Oncol* **35**: 608–611.

Igney FH, Krammer PH (2002). Death and anti-death: tumour resistance to apoptosis. *Nat Rev Cancer* **2**: 277–288.

Isoherranen N, Yagen B, Bialer M (2003). New CNS-active drugs which are second-generation valproic acid: can they lead to the development of a magic bullet? *Curr Opin Neurol* **16**: 203–211.

Kawagoe R, Kawagoe H, Sano K (2002). Valproic acid induces apoptosis in human leukemia cells by stimulating both caspase-dependent and -independent apoptotic signaling pathways. *Leuk Res* **26**: 495–502.

Komuro H, Hayashi Y, Kawamura M, Hayashi K, Kaneko Y, Kamoshita S *et al.* (1993). Mutations of the p53 gene are involved in Ewing's sarcomas but not in neuroblastomas. *Cancer Res* **53**: 5284–5288.

Laeng P, Pitts RL, Lemire AL, Drabik CE, Weiner A, Tang H *et al.* (2004). The mood stabilizer valproic acid stimulates GABA neurogenesis from rat forebrain stem cells. *J Neurochem* **91**: 238–251.

Legube G, Linares LK, Tyteca S, Caron C, Scheffner M, Chevillard-Briet M *et al*. (2004). Role of the histone acetyl transferase Tip60 in the p53 pathway. *J Biol Chem* **279**: 44825–44833.

Legube G, Trouche D (2003). Regulating histone acetyltransferases and deacetylases. *EMBO Rep* **4**: 944–947.

Lowe SW, Ruley HE, Jacks T, Housman DE (1993). p53-dependent apoptosis modulates the cytotoxicity of anticancer agents. *Cell* **74**: 957–967.

Mariadason JM, Barkla DH, Gibson PR (1997). Effect of short-chain fatty acids on paracellular permeability in Caco-2 intestinal epithelium model. *Am J Physiol* **272**: G705–G712.

Marks P, Rifkind RA, Richon VM, Breslow R, Miller T, Kelly WK (2001). Histone deacetylases and cancer: causes and therapies. *Nat Rev Cancer* **1**: 194–202.

Marzio G, Wagener C, Gutierrez MI, Cartwright P, Helin K, Giacca M (2000). E2F family members are differentially regulated by reversible acetylation. *J Biol Chem* **275**: 10887–10892.

Moll UM, LaQuaglia M, Benard J, Riou G (1995). Wild-type p53 protein undergoes cytoplasmic sequestration in undifferentiated neuroblastomas but not in differentiated tumors. *Proc Natl Acad Sci USA* **92**: 4407–4411.

Nicholson DW (2000). From bench to clinic with apoptosis-based therapeutic agents. *Nature* **407**: 810–816.

Phiel CJ, Zhang F, Huang EY, Guenther MG, Lazar MA, Klein PS (2001). Histone deacetylase is a direct target of valproic acid, a potent anticonvulsant, mood stabilizer, and teratogen. *J Biol Chem* **276**: 36734–36741.

Puthalakath H, Strasser A (2002). Keeping killers on a tight leash: transcriptional and post-translational control of the pro-apoptotic activity of BH3-only proteins. *Cell Death Differ* **9**: 505–512.

Reed JC, Meister L, Tanaka S, Cuddy M, Yum S, Geyer C *et al*. (1991). Differential expression of bcl2 protooncogene in neuroblastoma and other human tumor cell lines of neural origin. *Cancer Res* **51**: 6529–6538.

Savickiene J, Treigyte G, Borutinskaite V, Navakauskiene R, Magnusson KE (2006). The histone deacetylase inhibitor FK228 distinctly sensitizes the human leukemia cells to retinoic acid-induced differentiation. *Ann NY Acad Sci* **1091**: 368–384.

Schiavone N, Rosini P, Quattrone A, Donnini M, Lapucci A, Citti L *et al*. (2000). A conserved AU-rich element in the 3′ untranslated region of bcl-2 mRNA is endowed with a destabilizing function that is involved in bcl-2 down-regulation during apoptosis. *FASEB J* **14**: 174–184.

Sen S, D'Incalci M (1992). Apoptosis. Biochemical events and relevance to cancer chemotherapy. *FEBS Lett* **307**: 122–127.

Soengas MS, Capodieci P, Polsky D, Mora J, Esteller M, Opitz-Araya X *et al*. (2001). Inactivation of the apoptosis effector Apaf-1 in malignant melanoma. *Nature* **409**: 207–211.

Subramanian C, Opipari Jr AW, Bian X, Castle VP, Kwok RP (2005). Ku70 acetylation mediates neuroblastoma cell death induced by histone deacetylase inhibitors. *Proc Natl Acad Sci USA* **102**: 4842–4847.

Susin SA, Lorenzo HK, Zamzami N, Marzo I, Snow BE, Brothers GM *et al*. (1999). Molecular characterization of mitochondrial apoptosis-inducing factor. *Nature* **397**: 441–446.

Tweddle DA, Malcolm AJ, Bown N, Pearson AD, Lunec J (2001). Evidence for the development of p53 mutations after cytotoxic therapy in a neuroblastoma cell line. *Cancer Res* **61**: 8–13.

Vogan K, Bernstein M, Leclerc JM, Brisson L, Brossard J, Brodeur GM *et al*. (1993). Absence of p53 gene mutations in primary neuroblastomas. *Cancer Res* **53**: 5269–5273.

Waga S, Hannon GJ, Beach D, Stillman B (1994). The p21 inhibitor of cyclin-dependent kinases controls DNA replication by interaction with PCNA. *Nature* **369**: 574–578.

Waterhouse NJ, Ricci JE, Green DR (2002). And all of a sudden it's over: mitochondrial outer-membrane permeabilization in apoptosis. *Biochimie* **84**: 113–121.

Widlak P, Garrard WT (2005). Discovery, regulation, and action of the major apoptotic nucleases DFF40/CAD and endonuclease G. *J Cell Biochem* **94**: 1078–1087.

Willis SN, Adams JM (2005). Life in the balance: how BH3-only proteins induce apoptosis. *Curr Opin Cell Biol* **17**: 617–625.

Yuan PX, Huang LD, Jiang YM, Gutkind JS, Manji HK, Chen G (2001). The mood stabilizer valproic acid activates mitogen-activated protein kinases and promotes neurite growth. *J Biol Chem* **276**: 31674–31683.

Zhao Y, Lu S, Wu L, Chai G, Wang H, Chen Y *et al*. (2006). Acetylation of p53 at lysine 373/382 by the histone deacetylase inhibitor depsipeptide induces expression of p21(Waf1/Cip1). *Mol Cell Biol* **26**: 2782–2790.